

Trainable back-propagated functional transfer matrices

Cheng-Hao Cai^a, Yanyan Xu^{b,*}, Dengfeng Ke^c, Kaile Su^d, Jing Sun^a

^a*Department of Computer Science, The University of Auckland, 38 Princes Street, Auckland 1142, New Zealand*

^b*School of Information Science and Technology, Beijing Forestry University, 35 Qing-Hua East Road, Beijing 100083, China*

^c*National Laboratory of Pattern Recognition, Institute of Automation, Chinese Academy of Sciences, 95 Zhong-Guan-Cun East Road, Beijing 100190, China*

^d*Institute for Integrated and Intelligent Systems, Griffith University, 170 Kessels Road, Nathan, QLD 4111, Australia*

Abstract

Connections between nodes of fully connected neural networks are usually represented by weight matrices. In this article, functional transfer matrices are introduced as alternatives to the weight matrices: Instead of using real weights, a functional transfer matrix uses real functions with trainable parameters to represent connections between nodes. Multiple functional transfer matrices are then stacked together with bias vectors and activations to form deep functional transfer neural networks. These neural networks can be trained within the framework of back-propagation, based on a revision of the delta rules and the error transmission rule for functional connections. In experiments, it is demonstrated that the revised rules can be used to train a range of functional connections: 20 different functions are applied to neural networks with up to 10 hidden layers, and most of them gain high test accuracies on the MNIST database. It is also demonstrated that a functional transfer matrix with a memory function can roughly memorise a non-cyclical sequence of 400 digits.

Keywords: Functional Transfer Matrices, Deep learning, Trainable functional connections

*Corresponding author

Email addresses: chenghao.cai@outlook.com (Cheng-Hao Cai), xuyanyan@bjfu.edu.cn (Yanyan Xu), dengfeng.ke@nlpr.ia.ac.cn (Dengfeng Ke), k.su@griffith.edu.au (Kaile Su), j.sun@cs.auckland.ac.nz (Jing Sun)

1. Introduction

Many neural networks use weights to represent connections between nodes. For instance, a fully connected deep neural network usually has a weight matrix in each hidden layer, and the weight matrix, a bias vector and a nonlinear
 5 activation are used to map input signals to output signals [1]. Much work has been done on combining neural networks with different activations, such as the logistic function [2], the rectifier [3], the maxout function [4] and the long short-term memory blocks [5]. In this work, we study neural networks from another viewpoint: Instead of using different activations, we replace weights in
 10 the weight matrix with functional connections. In other words, the connections between nodes are represented by using real functions, but no longer real numbers. Specifically, this work focuses on:

- **Extending the back-propagation algorithm to the training of functional connections.** The extended back-propagation algorithm
 15 includes rules for computing deltas of parameters in functional connections and rules for transmitting error signals from a layer to its previous layer. This algorithm is adapted from the standard back-propagation algorithm for fully connected feedforward neural networks [6].
- **Discussing the meanings of some functionally connected structures.** Different functional transfer matrices can construct different
 20 mathematical structures. Although it is not necessary for these structures to have meanings, some of them do have meanings in practice.
- **Discussing some practical training methods for (deep) functional transfer neural networks.** Although the theory of back-propagation
 25 is applicable for these functional models, it is difficult to train them in practice. Also, the training becomes more difficult as the depth increases. In order to train them successfully, some tricks may be required.

- **Demonstrating that these functional transfer neural networks can practically work.** We apply these models to the MNIST handwritten digit dataset [7], in order to demonstrate that different functional connects can work for classification tasks. Also, we try to make a model with a memory function memorise the circumference ratio π , in order to demonstrate that functional connects can be used as a memory block.

The rest of this paper is organised as follows: Section 2 provides a brief review of the standard deep feedforward neural networks. Section 3 introduces the theory of functional transfer neural networks, including functional transfer matrices and a back-propagation algorithm for functional connections. Section 4 provides some examples for explaining the meanings of functionally connected structures. Section 5 discusses training methods for practical use. Section 6 provides experimental results. Section 7 introduces related work. Section 8 concludes this work and discusses future work.

2. Background on deep feedforward neural networks

We assume that readers have been familiar with deep feedforward neural networks and only mention concepts and formulae relevant to our research [6]: A feedforward neural network usually consists of an input layer, some hidden layers and an output layer. Two neighbouring layers are connected by a linear weight matrix \mathbf{W} , a bias vector \mathbf{b} and an activation φu . Given an vector \mathbf{x} , the neural network can map it to another vector \mathbf{y} via:

$$\mathbf{y} = \varphi(\mathbf{W} \cdot \mathbf{x} + \mathbf{b}) \quad . \quad (1)$$

3. A theory of functional transfer neural networks

3.1. Functional transfer matrices

Instead of using weights, a functional transfer matrix uses trainable functions to represent connections between nodes. Formally, it is defined as:

$$\mathbf{F} = \begin{pmatrix} F_{1,1}(x) & F_{1,2}(x) & \cdots & F_{1,n}(x) \\ F_{2,1}(x) & F_{2,2}(x) & \cdots & F_{2,n}(x) \\ \vdots & \vdots & \ddots & \vdots \\ F_{m,1}(x) & F_{m,2}(x) & \cdots & F_{m,n}(x) \end{pmatrix}, \quad (2)$$

where each $F_{i,j}(x)$ is a trainable function. We also define a transfer computation “ \odot ” for the functional transfer matrix and a column vector $\mathbf{v} = (v_1, v_2, \dots, v_n)^T$ such that:

$$\begin{aligned} \mathbf{F} \odot \mathbf{v} &= \begin{pmatrix} F_{1,1}(x) & F_{1,2}(x) & \cdots & F_{1,n}(x) \\ F_{2,1}(x) & F_{2,2}(x) & \cdots & F_{2,n}(x) \\ \vdots & \vdots & \ddots & \vdots \\ F_{m,1}(x) & F_{m,2}(x) & \cdots & F_{m,n}(x) \end{pmatrix} \odot \begin{pmatrix} v_1 \\ v_2 \\ \vdots \\ v_n \end{pmatrix} \\ &= \begin{pmatrix} F_{1,1}(v_1) + F_{1,2}(v_2) + \cdots + F_{1,n}(v_n) \\ F_{2,1}(v_1) + F_{2,2}(v_2) + \cdots + F_{2,n}(v_n) \\ \vdots \\ F_{m,1}(v_1) + F_{m,2}(v_2) + \cdots + F_{m,n}(v_n) \end{pmatrix}. \end{aligned} \quad (3)$$

Suppose that $\mathbf{b} = (b_1, b_2, \dots, b_m)^T$ is a bias vector, $\varphi(u)$ is an activation, and $\mathbf{x} = (x_1, x_2, \dots, x_n)^T$ is an input vector. An output vector $\mathbf{y} = (y_1, y_2, \dots, y_m)^T$ can then be computed via

$$\mathbf{y} = \varphi(\mathbf{F} \odot \mathbf{x} + \mathbf{b}). \quad (4)$$

In other words, the i th element of the output vector is

$$y_i = \varphi\left(\sum_{j=1}^n F_{i,j}(x_j) + b_i\right). \quad (5)$$

Multiple functional transfer matrices can be stacked together with bias vectors and activations to form a multi-layer model, and the model can be trained via back-propagation [6]: Suppose that a model has L hidden layers. For the l th hidden layer, $\mathbf{F}^{(l)}$ is a functional transfer matrix, its function $F_{i,j}^{(l)}(x)$ is a real function with an independent variable x and r trainable parameters $p_{i,j,k}^{(l)} (k = 1, 2, \dots, r)$, $\mathbf{b}^{(l)} = (b_1^{(l)}, b_2^{(l)}, \dots, b_m^{(l)})^T$ is a bias vector, $\varphi^{(l)}(u)$ is an activation, and $\mathbf{x}^{(l)} = (x_1^{(l)}, x_2^{(l)}, \dots, x_n^{(l)})^T$ is an input signal. An output signal $\mathbf{y}^{(l)} = (y_1^{(l)}, y_2^{(l)}, \dots, y_m^{(l)})^T$ is computed via:

$$\mathbf{y}^{(l)} = \varphi^{(l)}(\mathbf{F}^{(l)} \odot \mathbf{x}^{(l)} + \mathbf{b}^{(l)}) . \quad (6)$$

The output signal is the input signal of the next layer. In other words, if $l \leq L$, then $\mathbf{y}^{(l)} = \mathbf{x}^{(l+1)}$. After an error signal is evaluated by an output layer and an error function (see Section 5.2), the parameters can be updated: Suppose that $\delta_m^{(l)} = (\delta_1^{(l)}, \delta_2^{(l)}, \dots, \delta_m^{(l)})^T$ is an error signal of output nodes, and ϵ is a learning rate. Let $u_i^{(l)} = \sum_{j=1}^n F_{i,j}^{(l)}(x_j^{(l)}) + b_i^{(l)}$. Deltas of the parameters are computed via:

$$\begin{aligned} \Delta p_{i,j,k}^{(l)} &= \epsilon \cdot \delta_i^{(l)} \cdot \frac{\partial y_i^{(l)}}{\partial p_{i,j,k}^{(l)}} \\ &= \epsilon \cdot \delta_i^{(l)} \cdot \frac{\partial y_i^{(l)}}{\partial u_i^{(l)}} \cdot \frac{\partial u_i^{(l)}}{\partial F_{i,j}^{(l)}(x_j^{(l)})} \cdot \frac{\partial F_{i,j}^{(l)}(x_j^{(l)})}{\partial p_{i,j,k}^{(l)}} \\ &= \epsilon \cdot \delta_i^{(l)} \cdot \frac{\partial \varphi^{(l)}(u_i^{(l)})}{\partial u_i^{(l)}} \cdot \frac{\partial F_{i,j}^{(l)}(x_j^{(l)})}{\partial p_{i,j,k}^{(l)}} . \end{aligned} \quad (7)$$

Deltas of the biases are the same as the conventional rule:

$$\begin{aligned} \Delta b_i^{(l)} &= \epsilon \cdot \delta_i^{(l)} \cdot \frac{\partial y_i^{(l)}}{\partial b_i^{(l)}} \\ &= \epsilon \cdot \delta_i^{(l)} \cdot \frac{\partial y_i^{(l)}}{\partial u_i^{(l)}} \cdot \frac{\partial u_i^{(l)}}{\partial b_i^{(l)}} \\ &= \epsilon \cdot \delta_i^{(l)} \cdot \frac{\partial \varphi^{(l)}(u_i^{(l)})}{\partial u_i^{(l)}} . \end{aligned} \quad (8)$$

An error signal of the $(l - 1)$ th layer is computed via:

$$\begin{aligned}
\delta_j^{(l-1)} &= \sum_{i=1}^m \delta_i^{(l)} \cdot \frac{\partial y_i^{(l)}}{\partial x_j^{(l)}} \\
&= \sum_{i=1}^m \delta_i^{(l)} \cdot \frac{\partial y_i^{(l)}}{\partial u_i^{(l)}} \cdot \frac{\partial u_i^{(l)}}{\partial F_{i,j}^{(l)}(x_j^{(l)})} \cdot \frac{\partial F_{i,j}^{(l)}(x_j^{(l)})}{\partial x_j^{(l)}} \\
&= \sum_{i=1}^m \delta_i^{(l)} \cdot \frac{\partial \varphi^{(l)}(u_i^{(l)})}{\partial u_i^{(l)}} \cdot \frac{\partial F_{i,j}^{(l)}(x_j^{(l)})}{\partial x_j^{(l)}} .
\end{aligned} \tag{9}$$

Please note that the computation of $\frac{\partial F_{i,j}^{(l)}(x_j^{(l)})}{\partial x_j^{(l)}}$ can be simplified as a transfer

computation: Let $\mathbf{F}'^{(l)}$ be a derivative matrix in which each element is $\frac{\partial F_{i,j}^{(l)}(x)}{\partial x}$. Then the computation can be done via $\mathbf{F}'^{(l)} \odot \mathbf{x}^{(l)}$. Similarly, the computation of $\frac{\partial F_{i,j}^{(l)}(x_j^{(l)})}{\partial p_{i,j,k}^{(l)}}$ in Eq. (7) can also be simplified: Let $\mathbf{F}_k'^{(l)}$ be a derivative matrix

in which each element is $\frac{\partial F_{i,j}^{(l)}(x)}{\partial p_{i,j,k}^{(l)}}$. Then the computation can be done via $\mathbf{F}_k'^{(l)} \odot \mathbf{x}^{(l)}$. Both $\mathbf{F}'^{(l)}$ and $\mathbf{F}_k'^{(l)}$ can be computed symbolically before applying the transfer computation.

4. Examples

4.1. Periodic functions

Periodic functions can be applied to functional transfer matrices. For instance, $f(x) = A \cdot \sin(\omega \cdot x + \mu)$ is a periodic function, where A , ω and μ are its amplitude, angular velocity and initial phase respectively. Thus, we can define a matrix consisting of the following function:

$$F_{i,j}(x) = p_{i,j,1} \cdot \sin(p_{i,j,2} \cdot x + p_{i,j,3}) , \tag{10}$$

where $p_{i,j,1}$, $p_{i,j,2}$ and $p_{i,j,3}$ are trainable parameters. If it is an $M \times N$ matrix, then it can transfer an N -dimensional vector $(v_1, v_2, \dots, v_N)^T$ to an M -dimensional vector $(u_1, u_2, \dots, u_M)^T$ such that $u_i = \sum_{j=1}^N p_{i,j,1} \cdot \sin(p_{i,j,2} \cdot v_j + p_{i,j,3})$.

$v_j + p_{i,j,3}$). It is noticeable that each u_i is a composition of many periodic functions, and their amplitudes, angular velocities and initial phases can be updated via training. The training process is based on the following partial derivatives:

$$\frac{\partial F_{i,j}(x)}{\partial p_{i,j,1}} = \sin(p_{i,j,2} \cdot x + p_{i,j,3}) \quad , \quad (11)$$

$$\frac{\partial F_{i,j}(x)}{\partial p_{i,j,2}} = p_{i,j,1} \cdot \cos(p_{i,j,2} \cdot x + p_{i,j,3}) \cdot x \quad , \quad (12)$$

$$\frac{\partial F_{i,j}(x)}{\partial p_{i,j,3}} = p_{i,j,1} \cdot \cos(p_{i,j,2} \cdot x + p_{i,j,3}) \quad , \quad (13)$$

$$\frac{\partial F_{i,j}(x)}{\partial x} = p_{i,j,1} \cdot p_{i,j,2} \cdot \cos(p_{i,j,2} \cdot x + p_{i,j,3}) \quad , \quad (14)$$

55 Similarly, this method can be extended to the cosine function.

4.2. Modelling of conic hypersurfaces

A functional transfer neural network can represent decision boundaries constructed by ellipses and hyperbolas. Recall the mathematical definition of ellipses: A ellipse with a centre (c_1, c_2) and semi-axes a_1 and a_2 can be defined as $\frac{(x_1 - c_1)^2}{a_1^2} + \frac{(x_2 - c_2)^2}{a_2^2} = 1$. This equation can be rewritten

to $r \cdot \left(\frac{1}{a_1}\right)^2 \cdot (x_1 - c_1)^2 + r \cdot \left(\frac{1}{a_2}\right)^2 \cdot (x_2 - c_2)^2 + (-r) = 0$, where r is a

positive number. Let $p_1^2 = r \cdot \left(\frac{1}{a_1}\right)^2$, $p_2^2 = r \cdot \left(\frac{1}{a_2}\right)^2$, $q_1 = c_1$, $q_2 = c_2$ and $b = -r$. The equation becomes $p_1^2 \cdot (x_1 - q_1)^2 + p_2^2 \cdot (x_2 - q_2)^2 + b = 0$.

It is noticeable that $p_1^2 \cdot (x_1 - q_1)^2 + p_2^2 \cdot (x_2 - q_2)^2$ can be rewritten to

$(p_1^2 \cdot (x - q_1)^2 \quad p_2^2 \cdot (x - q_2)^2) \odot \begin{pmatrix} x_1 \\ x_2 \end{pmatrix}$, which is a transfer computation

(See Eq. 3). Therefore, a model with an activation $\xi(u)$ can be defined as

$y = \xi((p_1^2 \cdot (x - q_1)^2 \quad p_2^2 \cdot (x - q_2)^2) \odot \begin{pmatrix} x_1 \\ x_2 \end{pmatrix} + b)$ where x_1 and x_2 are inputs

and y is an output. Based on the above structure, multiple ellipse decision boundaries can be formed. For instance:

$$\begin{pmatrix} y_1 \\ y_2 \\ y_3 \end{pmatrix} = \xi \left(\begin{pmatrix} 0.50^2 \cdot (x - 2.00)^2 & 1.41^2 \cdot (x - 3.00)^2 \\ 1.33^2 \cdot (x - 2.50)^2 & 0.67^2 \cdot (x - 2.00)^2 \\ 1.00^2 \cdot (x - 3.00)^2 & 1.00^2 \cdot (x - 4.00)^2 \end{pmatrix} \odot \begin{pmatrix} x_1 \\ x_2 \end{pmatrix} + \begin{pmatrix} -1.00 \\ -1.00 \\ -1.00 \end{pmatrix} \right) , \quad (15)$$

$$z = \xi \left(\begin{pmatrix} -1.00 & -1.00 & -1.00 \end{pmatrix} \cdot \begin{pmatrix} y_1 \\ y_2 \\ y_3 \end{pmatrix} + 2.50 \right) , \quad (16)$$

and

$$\xi(x) = \begin{cases} 1, & x \geq 0 \\ 0, & x < 0 \end{cases} . \quad (17)$$

In the above model, x_1 and x_2 are input nodes. y_1 , y_2 and y_3 are hidden nodes. z is an output node. $\xi(x)$ is an activation. The input nodes and the hidden nodes are connected via a functional transfer matrix. The hidden nodes and the output node are connected via a weight matrix. The hidden nodes and the output node are activated via biases and the activation. Fig. 1 shows decision boundaries formed by this model: The functional transfer matrix and the hidden nodes form three ellipse boundaries (in orange, green and purple respectively). The weight matrix and the output node form a boundary which is the union of inner parts of all ellipse boundaries. In addition, this figure shows some example inputs and outputs: If the inputs are inside the decision boundaries, the output is 1. Otherwise, the output is 0. The reason why the model can construct ellipse boundaries is that its functional transfer matrix consists of the following function:

$$F_{i,j}(x) = p_{i,j,1}^2 \cdot (x - p_{i,j,2})^2 , \quad (18)$$

where $p_{i,j,1}$ and $p_{i,j,2}$ are trainable parameters. If the input dimension of this matrix is 2, it will construct ellipse boundaries on a plane. If its input dimension is 3, it will construct ellipsoid boundaries in a 3-dimensional space. Generally, if

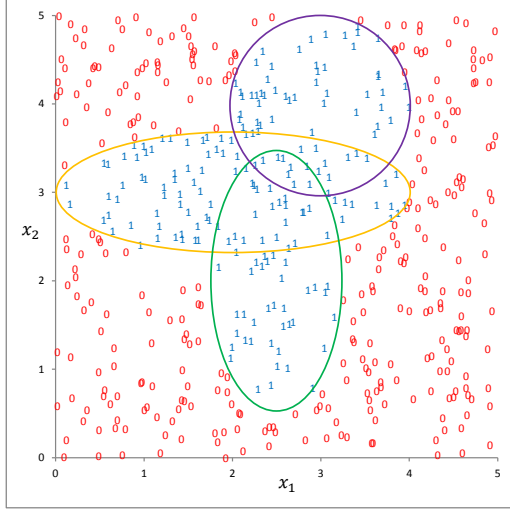


Figure 1: Decision boundaries formed by Eq. (15), Eq. (16) and Eq. (17).

its input dimension is N ($N \geq 2$), it will construct boundaries represented by $(N - 1)$ -dimensional closed hypersurfaces of ellipses in an N -dimensional space. This phenomenon reflects a significant difference between the a transfer matrix with Eq. (18) and a standard linear weight matrix, as the former models closed hypersurfaces, while the later models hyperplanes. In addition, to use the back-propagation algorithm to train the parameters, derivatives are computed via:

$$\frac{\partial F_{i,j}(x)}{\partial p_{i,j,1}} = 2 \cdot p_{i,j,1} \cdot (x - p_{i,j,2})^2 \quad , \quad (19)$$

$$\frac{\partial F_{i,j}(x)}{\partial p_{i,j,2}} = -2 \cdot p_{i,j,1}^2 \cdot (x - p_{i,j,2}) \quad , \quad (20)$$

$$\frac{\partial F_{i,j}(x)}{\partial x} = 2 \cdot p_{i,j,1}^2 \cdot (x - p_{i,j,2}) \quad , \quad (21)$$

Further, an adapted version of Eq. (18) can represent not only ellipses, but also hyperbolas. The adapted function is defined as:

$$F_{i,j}(x) = p_{i,j,1}^2 \cdot (x - p_{i,j,2})^2 \cdot u_{i,j} \quad , \quad (22)$$

where $u_{i,j}$ is initialised as 1 or -1. Please note that $u_{i,j}$ is a constant, but NOT a trainable parameter. Given a 1×2 matrix with this function:

$$\mathbf{F}_{conic} = \begin{pmatrix} p_{1,1,1}^2 \cdot (x - p_{1,1,2})^2 \cdot u_{1,1} & p_{1,2,1}^2 \cdot (x - p_{1,2,2})^2 \cdot u_{1,2} \end{pmatrix} . \quad (23)$$

If it is initialised by:

$$\begin{pmatrix} u_{1,1} & u_{1,2} \end{pmatrix} = \begin{pmatrix} 1 & 1 \end{pmatrix} , \quad (24)$$

then it can represent an ellipse boundary. On the other hand, if it is initialised by:

$$\begin{pmatrix} u_{1,1} & u_{1,2} \end{pmatrix} = \begin{pmatrix} 1 & -1 \end{pmatrix} , \quad (25)$$

then it can be used to form an hyperbola boundary. More generally, in an N -dimensional space, an $M \times N$ functional transfer matrix with Eq. (22) can represent M different $(N - 1)$ -dimensional conic hypersurfaces.

60 4.3. Sleeping weights and dead weights

In a standard neural network, connections between nodes usually do not “sleep”. The reason is that the connection from Node j to Node i is a real weight $w_{i,j}$. Let x_j denote a state of Node j . Node i will receive a signal $w_{i,j} \cdot x_j$. When $w_{i,j} \neq 0$ and $x_j \neq 0$, the signal always influences Node i , regardless of whether or not Node i needs it. To enable the connections to “sleep” temporarily, the following function is used in a functional transfer matrix:

$$F_{i,j}(x) = rect(p_{i,j,1} \cdot x + p_{i,j,2}) \cdot u_{i,j} . \quad (26)$$

In the above function, $p_{i,j,1}$ and $p_{i,j,2}$ are trainable parameters, and $u_{i,j}$ is a constant which is initialised as 1 or -1 before training. It also makes use of the rectifier [3]:

$$rect(x) = \begin{cases} x, & x \geq 0 \\ 0, & x < 0 \end{cases} . \quad (27)$$

The rectifier makes the function be able to “sleep”. In other words, when $p_{i,j,1} \cdot x + p_{i,j,2} \leq 0$, $F_{i,j}(x)$ must be zero. To use the back-propagation algorithm

to train the parameters, derivatives are computed via:

$$\frac{\partial F_{i,j}(x)}{\partial p_{i,j,1}} = \begin{cases} u_{i,j} \cdot x, & p_{i,j,1} \cdot x + p_{i,j,2} \geq 0 \\ 0, & p_{i,j,1} \cdot x + p_{i,j,2} < 0 \end{cases}, \quad (28)$$

$$\frac{\partial F_{i,j}(x)}{\partial p_{i,j,2}} = \begin{cases} u_{i,j}, & p_{i,j,1} \cdot x + p_{i,j,2} \geq 0 \\ 0, & p_{i,j,1} \cdot x + p_{i,j,2} < 0 \end{cases}, \quad (29)$$

$$\frac{\partial F_{i,j}(x)}{\partial x} = \begin{cases} p_{i,j,1} \cdot u_{i,j}, & p_{i,j,1} \cdot x + p_{i,j,2} \geq 0 \\ 0, & p_{i,j,1} \cdot x + p_{i,j,2} < 0 \end{cases}. \quad (30)$$

Another function enables a connection between two nodes to “die”. The word “die” is different from the word “sleep”, as the former means that $F_{i,j}(x) = 0$ for all x , and the later means that $F_{i,j}(x) = 0$ for some x . If the connection from Node j to Node i is dead, then any change of Node j does not influence Node i . This function is:

$$F_{i,j}(x) = \text{rect}(p_{i,j}) \cdot u_{i,j} \cdot x. \quad (31)$$

In the above function, $p_{i,j}$ is a trainable parameter, and $u_{i,j}$ is a constant which is initialised as 1 or -1 before training. To use the back-propagation algorithm to train the parameters, derivatives are computed via:

$$\frac{\partial F_{i,j}(x)}{\partial p_{i,j}} = \begin{cases} u_{i,j} \cdot x, & p_{i,j} \geq 0 \\ 0, & p_{i,j} < 0 \end{cases}, \quad (32)$$

$$\frac{\partial F_{i,j}(x)}{\partial x} = \text{rect}(p_{i,j}) \cdot u_{i,j}. \quad (33)$$

It is noticeable that $F_{i,j}(x)$, $\frac{\partial F_{i,j}(x)}{\partial p_{i,j}}$ and $\frac{\partial F_{i,j}(x)}{\partial x}$ are zero when $p_{i,j} < 0$, which means that the function does not transfer any signal and cannot be updated in this case. In other words, the function is dead once $p_{i,j}$ is updated to a negative value. A matrix with this function can then represent a partially connected neural network, as dead functions can be considered as broken connections after

training. A problem about the function is that it is not able to “revive”. In other words, once $p_{i,j}$ is updated to a negative value, it has no chance to be non-negative again. To solve this problem, an adapted version of the rectifier is used:

$$\text{rect}_{ada}(x) = \begin{cases} x, & x \geq 0 \\ 0, & x < 0 \end{cases} . \quad (34)$$

For the computation of $\frac{\partial F_{i,j}(x)}{\partial x}$, its derivative is:

$$\frac{\partial \text{rect}_{ada}(x)}{\partial x} = \begin{cases} 1, & x \geq 0 \\ 0, & x < 0 \end{cases} . \quad (35)$$

For the computation of $\frac{\partial F_{i,j}(x)}{\partial p_{i,j}}$, however, its derivative is arbitrarily defined as:

$$\frac{\partial \text{rect}_{ada}(x)}{\partial x} \equiv 1 . \quad (36)$$

We use “ \equiv ” instead of “=” because this derivative is not a mathematically sound result, but a predefined value. Thus, derivatives of $F_{i,j}(x)$ are computed via:

$$\frac{\partial F_{i,j}(x)}{\partial p_{i,j}} = u_{i,j} \cdot x , \quad (37)$$

$$\frac{\partial F_{i,j}(x)}{\partial x} = \begin{cases} u_{i,j}, & p_{i,j} \geq 0 \\ 0, & p_{i,j} < 0 \end{cases} . \quad (38)$$

It is noticeable that $\frac{\partial F_{i,j}(x)}{\partial p_{i,j}}$ is not zero when x is not zero, which means that $p_{i,j}$ can be updated when it is negative. Thus, although the function is dead when $p_{i,j}$ is negative, it can be revived by updating $p_{i,j}$ to a non-negative value.

4.4. Sequential Modelling via Memory Functions

A functional transfer matrix with memory functions can be used to model sequences. For instance, given a sequential input $\mathbf{x} = \{x_1, x_2, \dots, x_T\}$, the t th

state ($t = 1, 2, \dots, T$) of a memory function $F_{i,j}(x_t)$ is computed via:

$$F_{i,j}(x_t) = \tanh(p_{i,j,1} \cdot x_t + p_{i,j,2} \cdot C_{i,j,t-1} + p_{i,j,3}) \quad , \quad (39)$$

$$C_{i,j,t} = F_{i,j}(x_t) \quad , \quad (40)$$

where $p_{i,j,1}$, $p_{i,j,2}$ and $p_{i,j,3}$ are trainable parameters. In particular, $C_{i,j,t}$ is a memory cell and its initial state $C_{i,j,0}$ is set to 0. To use the back-propagation algorithm to train the parameters, derivatives are computed via:

$$\frac{\partial F_{i,j}(x_t)}{\partial p_{i,j,1}} = (1 - \tanh(p_{i,j,1} \cdot x_t + p_{i,j,2} \cdot C_{i,j,t-1} + p_{i,j,3})^2) \cdot x_t \quad , \quad (41)$$

$$\frac{\partial F_{i,j}(x_t)}{\partial p_{i,j,2}} = (1 - \tanh(p_{i,j,1} \cdot x_t + p_{i,j,2} \cdot C_{i,j,t-1} + p_{i,j,3})^2) \cdot C_{i,j,t-1} \quad , \quad (42)$$

$$\frac{\partial F_{i,j}(x_t)}{\partial p_{i,j,3}} = 1 - \tanh(p_{i,j,1} \cdot x_t + p_{i,j,2} \cdot C_{i,j,t-1} + p_{i,j,3})^2 \quad , \quad (43)$$

$$\frac{\partial F_{i,j}(x_t)}{\partial x_t} = (1 - \tanh(p_{i,j,1} \cdot x_t + p_{i,j,2} \cdot C_{i,j,t-1} + p_{i,j,3})^2) \cdot p_{i,j,1} \quad . \quad (44)$$

65 An $N \times M$ dimensional matrix with the memory function can record $N \times M$ signals from a previous state, as each memory function records one signal. On the other hand, a standard recurrent neural network usually uses hidden units to record signals from the previous state. If it has N input units and M hidden units, then it can record M signals. It is noticeable that the functional transfer
70 matrix with the memory function records $N - 1$ times more signals than the recurrent neural network.

5. Practical training methods for functional transfer neural networks

This section discusses some practical training methods for functional transfer neural networks. These methods are also used in the experiments (Section 6).

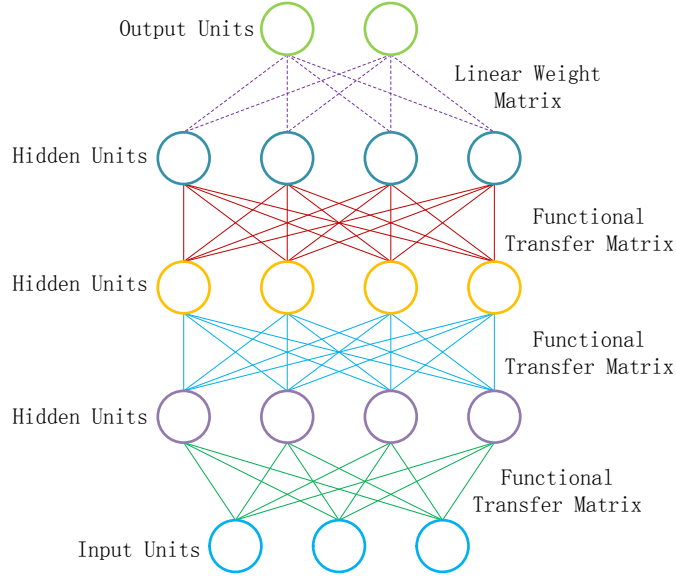


Figure 2: The general structure of functional transfer neural networks.

75 5.1. *The model structure and initialisation*

Fig. 2 shows the general structure of functional transfer neural networks: They usually have an input layer, one or more hidden layers and an output layer. Each hidden layer consists of a functional transfer matrix and some hidden units with a bias vector and an activation function. In particular, the activation function can be the logistic sigmoid function [3]:

$$\text{logistic}(u) = \frac{1}{1 + e^{-u}} \quad , \quad (45)$$

the rectified linear unit (ReLU)

$$\text{relu}(u) = \begin{cases} u, & u \geq 0 \\ 0, & u < 0 \end{cases} \quad , \quad (46)$$

or the hyperbolic tangent (tanh) function

$$\text{tanh}(u) = \frac{e^u - e^{-u}}{e^u + e^{-u}} \quad . \quad (47)$$

The output layer consists of a linear weight matrix and N output units with a bias vector and a softmax function:

$$\text{softmax}(u_i) = \frac{e^{u_i}}{\sum_{k=1}^N e^{u_k}} . \quad (48)$$

After setting up a model based on the above structure, parameters are initialised based on the following method:

- Weights in the linear weight matrix are randomised as small real numbers.
- Biases in the bias vectors are set to zero.
- 80 • For different functional transfer matrices, different initialisation methods should be used. In the experimental section, some examples of initialisation are provided (see Table 1 and Table 2).

5.2. Training a single hidden layer

If a model only has one hidden layer, the training can be done via back-
85 propagation directly [8]: Firstly, an input signal is propagated to the output layer, and an output signal is generated. Then an error signal is computed by comparing the output signal with a target signal. The comparison is based on the cross-entropy criterion [9]. Next, the error signal is back-propagated through the output layer and the hidden layer, and deltas of parameters are computed.
90 For the output layer, the standard delta rules are used. For the hidden layer, the rules described by Section 3.2 are used. Finally, the parameters are updated according to their deltas. The above process can be combined with stochastic gradient descent [10].

5.3. Layer-wise supervised training and fine-tuning

95 Training a functional transfer neural network can be more difficult when the number of hidden layers increases. To resolve this problem, the combination

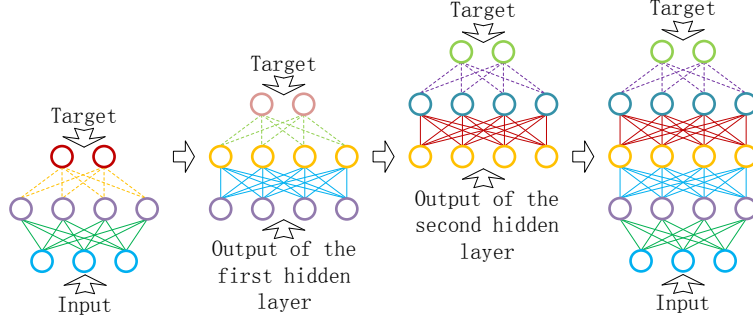


Figure 3: Layer-wise supervised training and fine-tuning. Functional connections are denoted by solid lines, and linear weight connections are denoted by dashed lines.

of layer-wise supervised training¹ and fine-tuning is used [11], which is shown by Fig. 3. Layer-wise training includes the following steps: Firstly, the first hidden layer is trained, while the other hidden layers and the output layer are ignored. To train this layer, a new softmax layer (with a linear weight matrix and a bias vector) is added onto it, and the method for training a single hidden layer (described by Section 5.2) is used to train it. Then the softmax layer is removed, and the second hidden layer is added onto the first hidden layer. To train the second hidden layer, another new softmax layer is added onto it, and the same training method is used again. Please note that the first hidden layer is not updated in this step. Finally, all remaining hidden layers are trained by using the same method. In particular, the trained softmax layer on the last hidden layer is considered as the output layer of the whole neural network. After layer-wise training, the whole neural network can be further optimised via fine-tuning: For the output layer, the standard back-propagation rules are used; For the hidden layers, the rules described by Section 3.2 are used. In practice, learning rates for fine-tuning are smaller than those for layer-wise training.

¹For details about layer-wise supervised training, please also refer to Algorithm 7 in the appendix of the referenced paper.

6. Experiments

6.1. MNIST handwritten digit recognition

115 6.1.1. Experimental settings

Table 1 provides 20 example functions which are used to construct functional transfer neural networks. $F_{i,j}(x)$ in the functional matrix (See Eq. (2)) is substituted for these example functions. In particular, $p_{i,j}$, $q_{i,j}$ and $r_{i,j}$ are used to denote trainable parameters instead of using $p_{i,j,k}$. These functions
120 include all functions discussed in Section 4, except the memory function in Section 4.4: F06, F07, and F08 have been discussed in Section 4.3; F12 has been discussed in Section 4.1; F19 and F20 have been discussed in Section 4.2. They also include functions which have not been discussed before, such as F01 - F05, F09 - F11 and F13 - F18. We test these examples to explore the
125 flexibility of the choice of functions. In fact, a wider range of functions may be useful, but it is difficult to cover all possible functions in this paper. On the other hand, some kinds of functions may not work. For instance, we have found that $F_{i,j}(x) = p_{i,j} \cdot \cosh(q_{i,j} \cdot x + r_{i,j})$ does not work, because the range of $f(x) = \cosh(x)$ is $[1, +\infty)$, which means that this function does not have a
130 “zero state”. To make it work, an additional “-1” should be used to change the range to $[0, +\infty)$, as indicated by F15. For another instance, $f(x) = \tan(x)$ does not work, because it is a discontinuous function. This is the reason why F12 cannot be changed to $F_{i,j}(x) = p_{i,j} \cdot \tan(q_{i,j} \cdot x + r_{i,j})$. For the same reason, some other discontinuous functions, including $f(x) = \cot(x)$, $f(x) = \sec(x)$,
135 $f(x) = \csc(x)$, $f(x) = \coth(x)$, $f(x) = \operatorname{sech}(x)$ and $f(x) = \operatorname{csch}(x)$, cannot be used in functional networks.

The model structure and the initialisation method have been revealed by Section 5.1. In particular, the input layer has 784 nodes, and the output layer has 10 nodes. They correspond to input pixels and output labels of the MNIST
140 database [7]. Besides, a model has 1, 5 or 10 hidden layers, and each hidden layer has 128 hidden units with the logistic activation, the ReLU or the tanh activation. Parameters of functional transfer matrices in these hidden layers

Table 1: Example Functions Used to Model Functional Networks.

ID	$F_{i,j}(x)$	Trainable Parameter(s)
F01	$p_{i,j}^2 \cdot x$	$p_{i,j}$
F02	$p_{i,j}^3 \cdot x$	$p_{i,j}$
F03	$p_{i,j} \cdot x^2 + q_{i,j} \cdot x$	$p_{i,j}, q_{i,j}$
F04	$p_{i,j} \cdot x^3 + q_{i,j} \cdot x^2 + r_{i,j} \cdot x$	$p_{i,j}, q_{i,j}, r_{i,j}$
F05	$p_{i,j} \cdot e^{q_{i,j} \cdot x}$	$p_{i,j}, q_{i,j}$
F06	$rect(p_{i,j}) \cdot u_{i,j} \cdot x$	$p_{i,j}$
F07	$rect_{ada}(p_{i,j}) \cdot u_{i,j} \cdot x$	$p_{i,j}$
F08	$rect(p_{i,j} \cdot x + q_{i,j}) \cdot u_{i,j}$	$p_{i,j}, q_{i,j}$
F09	$p_{i,j} \cdot rect(q_{i,j} \cdot x + r_{i,j})$	$p_{i,j}, q_{i,j}, r_{i,j}$
F10	$logistic(p_{i,j} \cdot x + q_{i,j}) \cdot u_{i,j}$	$p_{i,j}, q_{i,j}$
F11	$p_{i,j} \cdot logistic(q_{i,j} \cdot x + r_{i,j})$	$p_{i,j}, q_{i,j}, r_{i,j}$
F12	$p_{i,j} \cdot sin(q_{i,j} \cdot x + r_{i,j})$	$p_{i,j}, q_{i,j}, r_{i,j}$
F13	$p_{i,j} \cdot cos(q_{i,j} \cdot x + r_{i,j})$	$p_{i,j}, q_{i,j}, r_{i,j}$
F14	$p_{i,j} \cdot sinh(q_{i,j} \cdot x + r_{i,j})$	$p_{i,j}, q_{i,j}, r_{i,j}$
F15	$p_{i,j} \cdot (cosh(q_{i,j} \cdot x + r_{i,j}) - 1)$	$p_{i,j}, q_{i,j}, r_{i,j}$
F16	$p_{i,j} \cdot tanh(q_{i,j} \cdot x + r_{i,j})$	$p_{i,j}, q_{i,j}, r_{i,j}$
F17	$p_{i,j}^2 \cdot x^2$	$p_{i,j}$
F18	$p_{i,j}^2 \cdot x^2 \cdot u_{i,j}$	$p_{i,j}$
F19	$p_{i,j}^2 \cdot (x - q_{i,j})^2$	$p_{i,j}, q_{i,j}$
F20	$p_{i,j}^2 \cdot (x - q_{i,j})^2 \cdot u_{i,j}$	$p_{i,j}, q_{i,j}$

Table 2: Initialisation of Transfer Matrices.

ID	Initialisation Range
F05	$-0.1 \leq p_{i,j} \leq 0.1, -4.0 \leq q_{i,j} \leq -2.0$
F06	$0 \leq p_{i,j} \leq 2.0, u_{i,j} \in \{-1, 1\}$
F07	$0 \leq p_{i,j} \leq 2.0, u_{i,j} \in \{-1, 1\}$
F08	$-0.1 \leq p_{i,j} \leq 0.1, -0.1 \leq q_{i,j} \leq 0.1, u_{i,j} \in \{-1, 1\}$
F10	$-0.1 \leq p_{i,j} \leq 0.1, -0.1 \leq q_{i,j} \leq 0.1, u_{i,j} \in \{-1, 1\}$
F12	$-0.1 \leq p_{i,j} \leq 0.1, -10.0 \leq q_{i,j} \leq 10.0, -10.0 \leq r_{i,j} \leq 10.0$
F13	$-0.1 \leq p_{i,j} \leq 0.1, -10.0 \leq q_{i,j} \leq 10.0, -10.0 \leq r_{i,j} \leq 10.0$
F18	$-0.1 \leq p_{i,j} \leq 0.1, u_{i,j} \in \{-1, 1\}$
F20	$-0.1 \leq p_{i,j} \leq 0.1, -0.1 \leq q_{i,j} \leq 0.1, u_{i,j} \in \{-1, 1\}$
Others	$-0.1 \leq para \leq 0.1$, where <i>para</i> denotes $p_{i,j}$, $q_{i,j}$ or $r_{i,j}$.

are initialised based on Table 2. All training processes make use of the layer-wise supervised training and fine-tuning strategy discussed in Section 5.3. In particular, for layer-wise supervised training, the number of epochs is set to 15, and the learning rate is set to a constant 2^γ , where $\gamma \in \{0, -1, -2, -3, -4, -5\}$. For fine-tuning, the Newbob+/Train strategy is used [12]: The learning rate is set to $2^{\gamma-4}$ initially, and it will be halved if the improvement of the cross-entropy loss is smaller than 10^{-4} . The training stops when the improvement is smaller than zero, or after the 15th fine-tuning epoch. For both layer-wise training and fine-tuning, the size of mini-batches is set to 16.

6.1.2. Results

Table 3 shows test results of the models with 1 hidden layer. The results include accuracies after layer-wise training (LWT), accuracies after fine-tuning (FT) and the best γ for each model². Failed training cases are marked as “×”. In addition, F01 - F20 are IDs of functional transfer matrices, and Logistic,

²For full results of all γ values, please refer to Table 6 in Appendix.

Table 3: Accuracies (%) and the Best γ — 1 Hidden Layer.

Function	Logistic			ReLU			Tanh		
	LWT	FT	γ	LWT	FT	γ	LWT	FT	γ
F01	95.63	96.60	-1	96.30	96.73	-2	96.63	97.29	-1
F02	95.64	96.44	0	96.28	96.70	-1	96.67	96.81	-1
F03	97.98	98.04	0	98.04	98.05	-2	97.70	97.86	-4
F04	97.69	97.77	-2	97.98	97.98	-3	97.61	97.65	-4
F05	96.41	97.51	-3	96.49	97.63	-5	96.41	97.19	-5
F06	97.82	97.86	0	97.71	97.84	-3	97.64	97.76	-3
F07	97.99	97.99	0	98.05	98.12	-3	97.79	97.79	-2
F08	96.47	97.26	-2	95.77	97.22	-4	94.97	97.17	-4
F09	95.79	96.98	-1	96.38	97.46	-1	96.72	97.21	-2
F10	93.76	96.04	-1	94.81	96.65	-4	94.22	95.57	-4
F11	61.06	72.77	-4	×	×	×	76.36	88.92	-3
F12	96.84	97.08	-2	97.10	97.10	-3	96.51	96.61	-4
F13	96.53	96.90	-3	96.51	96.94	-5	96.41	96.80	-4
F14	95.82	97.00	0	96.91	97.49	-2	97.48	97.51	-1
F15	93.72	94.65	-1	91.74	94.44	-2	94.70	96.09	-1
F16	96.29	96.92	-1	96.04	97.56	-2	96.79	97.30	-2
F17	95.65	96.54	-1	94.68	96.29	-2	96.83	97.34	-2
F18	97.16	97.47	0	97.60	97.60	-1	97.02	97.16	-2
F19	94.68	96.84	-1	96.45	96.51	-1	97.01	97.43	-2
F20	97.67	97.88	0	97.87	97.90	-1	97.04	97.47	-2

ReLU and Tanh are activations of hidden units. It is noticeable that most models are trained successfully, except the F11-ReLU model. Although this model fails to be trained, its counterparts, including the F11-Logistic model and the F11-Tanh model, are trained successfully. Also, it is noticeable that the best γ is different for different functions and activations, which means that the initial learning rate should be carefully selected for different models.

Table 4 shows test results of the models with 5 hidden layers³. There are 8 models failed to be trained, which means that training is becoming more difficult when the number of hidden layers increases. On the other hand, there are 52 models trained successfully, which demonstrates that the revised back-propagation rules for functional transfer matrices are able to work for deep models. Among these models, 14 models obtain a better accuracy (after fine-tuning) than their counterparts in Table 3, whereas 38 models obtain a worse accuracy. Therefore, no evidence can show that more hidden layers must be better than less hidden layers, and vice versa. In addition, for a certain function, the best γ for ReLU is usually smaller than that for Logistic, and the best γ for Tanh is always smaller than that for Logistic. A similar phenomenon about γ has also appeared in Table 3.

Table 5 shows test results of the models with 10 hidden layers⁴. There are 11 models failed to be trained and 49 models trained successfully, which means that the functional transfer matrices still can work when there are up to 10 hidden layers, but training has become more difficult. Among the models trained successfully, 12 models obtain a better accuracy (after fine-tuning) than their counterparts in Table 4, 36 models obtain a worse accuracy, and one model obtains the same accuracy. These results show again that increasing the number of hidden layers can (but not always) bring about a worse accuracy. In addition, a comparison among the γ values in Table 3, Table 4 and Table 5 reveals that the best γ values are influenced by the functional transfer matrices, the activations

³For full results, please refer to Table 7 in Appendix.

⁴For full results, please refer to Table 8 in Appendix.

Table 4: Accuracies (%) and the Best γ — 5 Hidden Layers.

Function	Logistic			ReLU			Tanh		
	LWT	FT	γ	LWT	FT	γ	LWT	FT	γ
F01	94.55	95.78	-2	95.82	96.04	-3	96.27	96.80	-3
F02	94.47	95.41	0	96.10	96.39	-2	95.93	96.40	-1
F03	98.08	98.10	-2	91.69	91.69	-5	97.92	97.92	-3
F04	97.73	97.78	-2	89.49	89.49	-5	97.90	97.93	-4
F05	97.45	97.55	-3	95.50	96.22	-5	×	×	×
F06	97.79	97.85	0	97.70	97.70	-3	97.91	97.91	-4
F07	97.92	97.92	0	97.58	97.58	-4	97.75	97.79	-3
F08	97.41	97.56	-2	97.30	97.37	-4	97.40	97.46	-4
F09	95.75	96.28	-1	97.39	97.54	-2	96.92	96.98	-2
F10	93.66	95.44	-1	96.60	96.89	-3	95.76	95.94	-3
F11	×	×	×	×	×	×	86.25	87.94	-3
F12	96.83	96.83	-2	93.62	93.62	-4	96.13	96.13	-4
F13	96.44	96.44	-2	94.03	94.03	-3	95.91	95.91	-4
F14	96.68	96.97	-1	×	×	×	97.35	97.41	-2
F15	87.68	93.17	-1	90.21	90.21	-3	95.45	96.00	-1
F16	96.72	96.73	-1	97.37	97.47	-3	97.32	97.38	-2
F17	93.98	95.37	-1	×	×	×	84.23	95.79	-3
F18	96.60	96.81	-1	×	×	×	61.73	96.20	-1
F19	94.33	96.41	-1	×	×	×	95.60	96.52	-2
F20	97.24	97.25	0	×	×	×	96.72	96.72	-1

Table 5: Accuracies (%) and the Best γ — 10 Hidden Layers.

Function	Logistic			ReLU			Tanh		
	LWT	FT	γ	LWT	FT	γ	LWT	FT	γ
F01	93.48	95.08	-2	95.81	95.91	-3	95.76	96.28	-3
F02	93.14	94.92	-1	96.07	96.65	-2	95.63	96.24	-2
F03	97.85	97.85	-2	\times	\times	\times	97.84	97.87	-4
F04	97.78	97.78	-1	\times	\times	\times	97.82	97.82	-2
F05	97.11	97.52	-3	95.15	95.92	-5	\times	\times	\times
F06	98.08	98.08	-1	97.50	97.55	-5	97.69	97.70	-3
F07	98.09	98.09	-1	97.64	97.72	-4	97.71	97.73	-4
F08	97.38	97.45	-2	97.26	97.27	-4	97.29	97.53	-4
F09	95.67	96.59	-1	96.96	97.31	-1	96.84	97.00	-2
F10	94.68	95.53	-1	96.66	96.94	-4	95.49	95.85	-3
F11	\times	\times	\times	\times	\times	\times	84.83	86.49	-4
F12	96.52	96.52	-2	91.63	91.63	-4	95.26	95.26	-4
F13	96.84	96.84	-2	92.20	92.20	-3	95.36	95.36	-4
F14	96.50	96.83	0	\times	\times	\times	97.09	97.37	-2
F15	83.40	90.20	-2	\times	\times	\times	94.12	94.12	-1
F16	96.22	96.70	-1	97.33	97.45	-1	96.88	97.13	-2
F17	93.44	95.21	-2	\times	\times	\times	71.84	95.60	-3
F18	96.40	96.84	-1	\times	\times	\times	60.29	95.82	-3
F19	93.75	94.80	-3	\times	\times	\times	95.44	95.44	-1
F20	97.11	97.41	-1	\times	\times	\times	96.03	96.03	-1

185 and the number of hidden layers, but it is difficult to find a way to predict them.
Therefore, tuning of γ is still required in practice.

6.2. Memorising the digits of π

6.2.1. Experimental settings

This is a short experiment to evaluate the memory function discussed
190 by Section 4.4, because it is a time-dependent function and cannot be
evaluated by using the same methodology as the previous experiments. In
this part, we explore if functional transfer neural networks with the memory
function are able to model the sequence of the circumference ratio⁵ $\pi =$
3.141592653589793238 \dots . Specifically, given the first $n - 1$ digits, the neural
195 networks are expected to output the n th digit. Each neural network has an
input layer, a hidden layer and an output layer: The input layer has 10 nodes
which correspond to digits 0, 1, 2, \dots , 9. The hidden layer has 128, 256, 512 or
1024 nodes, and it consists of a functional transfer matrix with the memory
function, a bias vector and a logistic activation. The output layer has 10
200 nodes which correspond to digits 0, 1, 2, \dots , 9, and it consists of a linear weight
matrix, a bias vector and a softmax activation. All trainable parameters in
the two matrices are initialised as a real number in $[-0.1, 0.1]$. All biases are
initialised as zero. The training method described by Section 5.2 is used to
train the models. Each training epoch makes use of a sequence of training pairs
205 $\langle x_i, x_{i+1} \rangle$ ($i = 1, 2, \dots, D$). For each training pair, x_i and x_{i+1} are one-
hot encodings of the i th and $(i + 1)$ th digits of π respectively. x_i is an input,
and x_{i+1} is a target of output. D is set to 200, 400 or 800. The number of
training epochs is set to 5000. The learning rate is set to 2^{-4} , and it is not
changed during the whole training process. Model performance is evaluated by
210 the accuracy of predicting x_{i+1} .

⁵ The circumference ratio is chosen as experimental data because it is an irrational
number, containing a non-cyclical sequence of digits. The dataset can be downloaded from
[https://github.com/cchrewrite/Functional-Transfer-Neural-Networks/blob/master/](https://github.com/cchrewrite/Functional-Transfer-Neural-Networks/blob/master/circumference-ratio-data.txt)
circumference-ratio-data.txt.

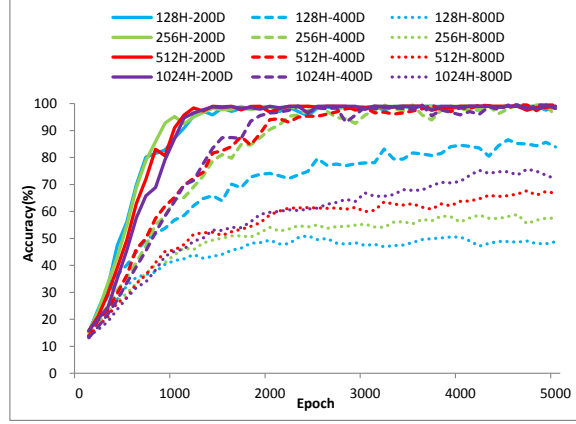


Figure 4: Learning curves of functional transfer neural networks with the memory function.

6.2.2. Results

Fig. 4 shows accuracies of the models with the memory function. Each model is denoted by “ $xH-yD$ ”, where x is the number of hidden units, and y the number of training pairs. It is noticeable that all 200D models gain high accuracies after the first 1500 training epochs, and the 256H-400D, 512H-400D and 1024H-400D models gain high accuracies after the first 2500 training epochs, which means that matrices with the memory function are able to model the sequence of digits. However, the 128H-400D model does not gain an accuracy as high as its counterparts, which means that its memory is restricted by the size of the matrix. In other words, to memorise a longer sequence, the number of hidden units should increase, because it determines the size of the functional transfer matrix and determines consequently the number of memory functions. For the 800D models, it is clear that the increase of the number of hidden units brings about better accuracies, though the accuracies are not significantly high.

7. Related work

In this section, some previous work about functional-link neural networks, deep neural networks and neurons are revised, and comparisons between them

and our work are carried out.

7.1. Functional-link neural networks

230 Functional-link neural networks use functional-links to enhance input patterns [13]. Usually, they consist of a functional expansion module, an input layer and an output layer, and the functional expansion module consists of many functional-links: For instance, a functional-link can be a trainable linear function (which is called a random variable functional-link), a multiplication
235 function (which is called a generic basis), a trigonometric function or a Chebyshev polynomial basis function [14]. A typical application of functional-link neural networks is to model nonlinear decision boundaries in channel equalisers [15]. Dehuri and Cho [16] also use them as classifiers, where functional-links are used to select input features.

240 There are four main differences between our work and the above work about functional-link neural networks: Firstly, we use functional transfer matrices as alternatives to standard weight matrices, whereas functional expansion modules are NOT alternatives to weight matrices in functional-link neural networks. Secondly, our models have up to 10 hidden layers, and functional transfer
245 matrices are applied to all of them, whereas functional-link neural networks have no hidden layer or have only one hidden layer with a linear weight matrix, and functional-links are only used to enhance input patterns [16, 13]. Thirdly, most functional transfer matrices are trainable, whereas most functional-links are fixed (except the random variable functional-link). Finally, functional transfer
250 matrices are applied to hand-written digit recognition and the modelling of memory blocks, and they are different from the applications of functional-links.

7.2. Deep architecture

Deep architecture has been applied to many fields. For instance, it can be used to map pixels to a symbol [3, 17], map a frame of voice to a phone [1, 18],
255 model a sentence to a feature [19], decide how to use a logical rule for automated theorem proving [20, 21], manipulate variables in symbolic representations [22],

guide the synthesis of programs [23], etc. In the above applications, deep neural networks play a role that maps input signals with different sizes, shapes and structures to vectorised features. Similarly, the first part of our experiments
260 also focuses on this aspect: Neural networks with functional transfer matrices are used to map pixels to vectorised features.

7.3. *The improvement of neurons*

In a feedforward neural network, neurons (activations) in hidden layers are originally the logistic function [24]. The logistic function can be replaced with
265 the tanh function, the softsign function, the ReLU, the softplus function, the maxout function, or the soft-maxout function [3, 25, 26]. Also, neurons can be more complicated: For instance, they can be Clifford neurons in hyperconformal space and be used to construct ellipsoidal hypersurfaces [27]. The Clifford neurons are based on the Clifford algebra which extends multiplications
270 of neural networks from real spaces to multi-dimensional geometric spaces [28]. Also, they can be the Taylor series of some simple activation functions, and the Taylor series can become trainable functions, because their coefficients can be trained [29]. Another kind of trainable neurons is called the Hermitian activation function [30]. The Hermitian activation function is applied to feedforward neural
275 networks with one hidden layer, and its shape can be changed by adapting its parameters [31]. Besides, neurons can be functions processing not only real numbers, but also complex numbers, according to the theory of complex back-propagation [32]: For instance, they can form multivalued neurons in feedforward neural networks [33]. They can also be extended to the hypercomplex domain and form quaternion neural networks, which can process input
280 elements with a scalar and three orthogonal vectors [34]. Further, they can be applied to not only fully connected neural networks, but also convolutional neural networks [35]. Different from the above work about neurons, our work focuses on improving the matrices between neurons instead of improving neurons
285 themselves.

8. Conclusion and future work

In this article, the theory and the applications of functional transfer matrices are presented. As argued in Section 3, connections between nodes of a fully connected neural network can be represented by trainable functional connections instead of standard weights, and the theory of back-propagation can be extended to the training of these functional connections. Different functional transfer matrices can form different mathematical structures, such as conic hypersurfaces, periodic functions, sleeping units and dead units. Also, multiple functional transfer matrices can form a deep structure called a deep functional transfer neural network, but the training becomes more difficult when the number of hidden layers increases. Practically, the use of layer-wise supervised training and fine-tuning can solve this problem. In the experiments, a wide range of functional transfer matrices are demonstrated to be trainable and be able to gain high test accuracies on the MNIST database. It is also demonstrated that the neural network with the memory function can roughly memorise hundreds of digits of the circumference ratio, which means that the neural network can memorise previous information and form a memory block. There also remain many possibilities worth exploring in the future: Firstly, it is possible to apply functional transfer matrices to other kinds of neural networks, such as recurrent neural networks and convolutional neural networks, because their weights may also be replaced with functional connections. Secondly, it is often possible to design functional connections for special purposes, as there are an infinite number of possible combinations of functions. Thirdly, the training of deep functional transfer neural networks still relies on the layer-wise approach. Is there any efficient and effect way to train all layers directly? Finally, it is possible to apply functional transfer matrices to more fields besides the two applications in this work. In summary, this article has carried out the concept and shown the viability of changing the structure of neural networks by replacing weights with functional connections, and it is believed that the use of functional connections can bring about more potential for neural networks.

Acknowledgement

Funding: This work was supported by the Fundamental Research Funds for the Central Universities [grant number 2016JX06]; and the National Natural Science Foundation of China [grant number 61472369].

References

References

- [1] A. Mohamed, G. E. Dahl, G. E. Hinton, Acoustic modeling using deep belief networks, *IEEE Trans. Audio, Speech & Language Processing* 20 (1) (2012) 14–22. doi:10.1109/TASL.2011.2109382.

URL <https://doi.org/10.1109/TASL.2011.2109382>

- [2] S. Dreiseitl, L. Ohno-Machado, Logistic regression and artificial neural network classification models: a methodology review, *Journal of Biomedical Informatics* 35 (5-6) (2002) 352–359. doi:10.1016/S1532-0464(03)00034-0.

URL [https://doi.org/10.1016/S1532-0464\(03\)00034-0](https://doi.org/10.1016/S1532-0464(03)00034-0)

- [3] X. Glorot, A. Bordes, Y. Bengio, Deep sparse rectifier neural networks, in: *Proceedings of the Fourteenth International Conference on Artificial Intelligence and Statistics, AISTATS 2011, Fort Lauderdale, USA, April 11-13, 2011, 2011*, pp. 315–323.

URL <http://www.jmlr.org/proceedings/papers/v15/glorot11a/glorot11a.pdf>

- [4] G. F. Montúfar, R. Pascanu, K. Cho, Y. Bengio, On the number of linear regions of deep neural networks, in: *Advances in Neural Information Processing Systems 27: Annual Conference on Neural Information Processing Systems 2014, December 8-13 2014, Montreal, Quebec, Canada, 2014*, pp. 2924–2932.

URL <http://papers.nips.cc/paper/5422-on-the-number-of-linear-regions-of-deep-neural-ne>

- [5] S. Hochreiter, J. Schmidhuber, Long short-term memory, *Neural Computation* 9 (8) (1997) 1735–1780. doi:10.1162/neco.1997.9.8.1735.
 345 URL <https://doi.org/10.1162/neco.1997.9.8.1735>
- [6] R. Hecht-Nielsen, Theory of the backpropagation neural network, *Neural Networks* 1 (Supplement-1) (1988) 445–448. doi:10.1016/0893-6080(88)90469-8.
 URL [https://doi.org/10.1016/0893-6080\(88\)90469-8](https://doi.org/10.1016/0893-6080(88)90469-8)
- [7] L. Deng, The MNIST database of handwritten digit images for machine learning research [best of the web], *IEEE Signal Process. Mag.* 29 (6) (2012) 141–142. doi:10.1109/MSP.2012.2211477.
 350 URL <https://doi.org/10.1109/MSP.2012.2211477>
- [8] D. E. Rumelhart, G. E. Hinton, R. J. Williams, et al., Learning representations by back-propagating errors, *Cognitive modeling* 5 (3) (1988) 1.
 355
- [9] G. Hinton, L. Deng, D. Yu, G. E. Dahl, A.-r. Mohamed, N. Jaitly, A. Senior, V. Vanhoucke, P. Nguyen, T. N. Sainath, et al., Deep neural networks for acoustic modeling in speech recognition: The shared views of four research groups, *IEEE Signal Processing Magazine* 29 (6) (2012) 82–97.
 360
- [10] M. Zinkevich, M. Weimer, A. J. Smola, L. Li, Parallelized stochastic gradient descent, in: *Advances in Neural Information Processing Systems* 23: 24th Annual Conference on Neural Information Processing Systems 2010. Proceedings of a meeting held 6-9 December 2010, Vancouver, British Columbia, Canada., 2010, pp. 2595–2603.
 365 URL <http://papers.nips.cc/paper/4006-parallelized-stochastic-gradient-descent>
- [11] Y. Bengio, P. Lamblin, D. Popovici, H. Larochelle, Greedy layer-wise training of deep networks, in: *Advances in Neural Information Processing Systems* 19, Proceedings of the Twentieth Annual Conference on Neural Information Processing Systems, Vancouver, British Columbia, Canada,
 370

December 4-7, 2006, 2006, pp. 153–160.

URL <http://papers.nips.cc/paper/3048-greedy-layer-wise-training-of-deep-networks>

- [12] S. Wiesler, A. Richard, R. Schlüter, H. Ney, Mean-normalized stochastic gradient for large-scale deep learning, in: IEEE International Conference on Acoustics, Speech and Signal Processing, ICASSP 2014, Florence, Italy, May 4-9, 2014, 2014, pp. 180–184. doi:10.1109/ICASSP.2014.6853582.
375 URL <http://dx.doi.org/10.1109/ICASSP.2014.6853582>
- [13] Y. Pao, G. H. Park, D. J. Sobajic, Learning and generalization characteristics of the random vector functional-link net, Neurocomputing
380 6 (2) (1994) 163–180. doi:10.1016/0925-2312(94)90053-1.
URL [https://doi.org/10.1016/0925-2312\(94\)90053-1](https://doi.org/10.1016/0925-2312(94)90053-1)
- [14] S. Dehuri, S. Cho, A comprehensive survey on functional link neural networks and an adaptive PSO-BP learning for CFLNN, Neural Computing and Applications 19 (2) (2010) 187–205. doi:10.1007/s00521-009-0288-5.
385 URL <https://doi.org/10.1007/s00521-009-0288-5>
- [15] H. Zhao, J. Zhang, Functional link neural network cascaded with chebyshev orthogonal polynomial for nonlinear channel equalization, Signal Processing 88 (8) (2008) 1946–1957. doi:10.1016/j.sigpro.2008.01.029.
390 URL <https://doi.org/10.1016/j.sigpro.2008.01.029>
- [16] S. Dehuri, S. Cho, Evolutionarily optimized features in functional link neural network for classification, Expert Syst. Appl. 37 (6) (2010) 4379–4391. doi:10.1016/j.eswa.2009.11.090.
395 URL <https://doi.org/10.1016/j.eswa.2009.11.090>
- [17] X. Glorot, Y. Bengio, Understanding the difficulty of training deep feedforward neural networks, in: Proceedings of the Thirteenth International Conference on Artificial Intelligence and Statistics, AISTATS

- 2010, Chia Laguna Resort, Sardinia, Italy, May 13-15, 2010, 2010, pp. 249–
 400 256.
 URL <http://www.jmlr.org/proceedings/papers/v9/glorot10a.html>
- [18] L. Deng, G. E. Hinton, B. Kingsbury, New types of deep neural network
 learning for speech recognition and related applications: an overview, in:
 IEEE International Conference on Acoustics, Speech and Signal Processing,
 405 ICASSP 2013, Vancouver, BC, Canada, May 26-31, 2013, 2013, pp. 8599–
 8603. doi:10.1109/ICASSP.2013.6639344.
 URL <https://doi.org/10.1109/ICASSP.2013.6639344>
- [19] R. Sarikaya, G. E. Hinton, A. Deoras, Application of deep belief networks
 for natural language understanding, IEEE/ACM Trans. Audio, Speech &
 410 Language Processing 22 (4) (2014) 778–784. doi:10.1109/TASLP.2014.
 2303296.
 URL <https://doi.org/10.1109/TASLP.2014.2303296>
- [20] G. Irving, C. Szegedy, A. A. Alemi, N. Eén, F. Chollet, J. Urban,
 Deepmath - deep sequence models for premise selection, in: Advances in
 415 Neural Information Processing Systems 29: Annual Conference on Neural
 Information Processing Systems 2016, December 5-10, 2016, Barcelona,
 Spain, 2016, pp. 2235–2243.
 URL [http://papers.nips.cc/paper/6280-deepmath-deep-sequence-models-for-premise-selecti](http://papers.nips.cc/paper/6280-deepmath-deep-sequence-models-for-premise-selection)
- [21] C. Cai, D. Ke, Y. Xu, K. Su, Learning of human-like algebraic reasoning
 420 using deep feedforward neural networks, CoRR abs/1704.07503.
 URL <http://arxiv.org/abs/1704.07503>
- [22] C. Cai, D. Ke, Y. Xu, K. Su, Symbolic manipulation based on deep neural
 networks and its application to axiom discovery, in: 2017 International
 Joint Conference on Neural Networks, IJCNN 2017, Anchorage, AK,
 425 USA, May 14-19, 2017, 2017, pp. 2136–2143. doi:10.1109/IJCNN.2017.
 7966113.
 URL <https://doi.org/10.1109/IJCNN.2017.7966113>

- [23] M. Balog, A. L. Gaunt, M. Brockschmidt, S. Nowozin, D. Tarlow, Deepcoder: Learning to write programs, CoRR abs/1611.01989.
 430 URL <http://arxiv.org/abs/1611.01989>
- [24] Y. LeCun, Y. Bengio, G. Hinton, Deep learning, Nature 521 (7553) (2015) 436–444.
- [25] J. Bergstra, G. Desjardins, P. Lamblin, Y. Bengio, Quadratic polynomials learn better image features, Tech. rep., Technical Report 1337,
 435 Département d’Informatique et de Recherche Opérationnelle, Université de Montréal (2009).
- [26] X. Zhang, J. Trmal, D. Povey, S. Khudanpur, Improving deep neural network acoustic models using generalized maxout networks, in: IEEE International Conference on Acoustics, Speech and Signal Processing, ICASSP 2014, Florence, Italy, May 4-9, 2014, 2014, pp. 215–219. doi:
 440 10.1109/ICASSP.2014.6853589.
 URL <https://doi.org/10.1109/ICASSP.2014.6853589>
- [27] C. Villaseñor, N. Arana-Daniel, A. Y. Alanis, C. López-Franco, Hyperellipsoidal neuron, in: 2017 International Joint Conference on Neural Networks, IJCNN 2017, Anchorage, AK, USA, May 14-19, 2017, 2017, pp. 788–794. doi:10.1109/IJCNN.2017.7965932.
 445 URL <https://doi.org/10.1109/IJCNN.2017.7965932>
- [28] S. Buchholz, G. Sommer, On clifford neurons and clifford multi-layer perceptrons, Neural Networks 21 (7) (2008) 925–935. doi:10.1016/j.neunet.2008.03.004.
 450 URL <https://doi.org/10.1016/j.neunet.2008.03.004>
- [29] H. Chung, S. J. Lee, J. G. Park, Deep neural network using trainable activation functions, in: 2016 International Joint Conference on Neural Networks, IJCNN 2016, Vancouver, BC, Canada, July 24-29, 2016, 2016, pp. 348–352. doi:10.1109/IJCNN.2016.7727219.
 455 URL <https://doi.org/10.1109/IJCNN.2016.7727219>

- [30] S. M. Siniscalchi, T. Svendsen, F. Sorbello, C. Lee, Experimental studies on continuous speech recognition using neural architectures with "adaptive" hidden activation functions, in: Proceedings of the IEEE International Conference on Acoustics, Speech, and Signal Processing, ICASSP 2010, 14-19 March 2010, Sheraton Dallas Hotel, Dallas, Texas, USA, 2010, pp. 4882–4885. doi:10.1109/ICASSP.2010.5495120.
URL <https://doi.org/10.1109/ICASSP.2010.5495120>
- [31] S. M. Siniscalchi, J. Li, C. Lee, Hermitian polynomial for speaker adaptation of connectionist speech recognition systems, IEEE Trans. Audio, Speech & Language Processing 21 (10) (2013) 2152–2161. doi:10.1109/TASL.2013.2270370.
URL <https://doi.org/10.1109/TASL.2013.2270370>
- [32] H. Leung, S. Haykin, The complex backpropagation algorithm, IEEE Trans. Signal Processing 39 (9) (1991) 2101–2104. doi:10.1109/78.134446.
URL <https://doi.org/10.1109/78.134446>
- [33] I. N. Aizenberg, C. Moraga, Multilayer feedforward neural network based on multi-valued neurons (MLMVN) and a backpropagation learning algorithm, Soft Comput. 11 (2) (2007) 169–183. doi:10.1007/s00500-006-0075-5.
URL <https://doi.org/10.1007/s00500-006-0075-5>
- [34] N. Matsui, T. Isokawa, H. Kusamichi, F. Peper, H. Nishimura, Quaternion neural network with geometrical operators, Journal of Intelligent and Fuzzy Systems 15 (3-4) (2004) 149–164.
URL <http://content.iospress.com/articles/journal-of-intelligent-and-fuzzy-systems/ifs00236>
- [35] Y. Kominami, H. Ogawa, K. Murase, Convolutional neural networks with multi-valued neurons, in: 2017 International Joint Conference on Neural Networks, IJCNN 2017, Anchorage, AK, USA, May 14-19, 2017, 2017, pp.

2673–2678. doi:10.1109/IJCNN.2017.7966183.

URL <https://doi.org/10.1109/IJCNN.2017.7966183>

Appendix

The appendix provides full results of the experiments in Section 6.1: Table
490 6, Table 7 and Table 8 shows test accuracies of models with 1, 5 and 10 hidden
layers respectively. In these tables, accuracies are recorded as x/y , where x
denotes an accuracy after layer-wise supervised training, and y denotes an
accuracy after fine-tuning. In particular, “ \times ” means that a model fails to be
trained. To reduce the size of tables, “Activation” is abbreviated to “Act.”, and
495 the logistic sigmoid function is abbreviated to “LogS”.

Table 6: Full Results on MNIST — 1 Hidden Layer

ID	Act.	$\gamma = 0$	$\gamma = -1$	$\gamma = -2$	$\gamma = -3$	$\gamma = -4$	$\gamma = -5$
F01	LogS	93.70/96.18	95.63/96.60	95.89/96.40	95.06/95.75	94.43/94.95	92.58/93.03
	ReLU	94.26/94.51	96.51/96.66	96.30/96.73	94.96/95.77	93.33/93.91	92.06/92.23
	Tanh	96.61/96.67	96.63/97.29	96.56/97.29	96.91/97.15	96.00/96.17	94.89/94.89
F02	LogS	95.64/96.44	95.24/95.80	94.36/94.59	92.85/93.18	89.92/90.21	85.99/86.36
	ReLU	74.19/75.23	96.28/96.70	95.20/95.98	94.76/95.43	93.25/93.55	90.69/91.21
	Tanh	95.55/95.93	96.67/96.81	96.16/96.54	95.38/95.78	94.62/94.71	92.18/92.25
F03	LogS	97.98/98.04	97.83/97.86	97.63/97.65	97.75/97.75	97.08/97.19	96.31/96.39
	ReLU	x	x	98.04/98.05	97.91/97.92	97.98/97.98	97.70/97.88
	Tanh	42.22/48.03	97.10/97.10	97.80/97.80	97.64/97.67	97.70/97.86	97.55/97.64
F04	LogS	97.76/97.76	97.72/97.76	97.69/97.77	97.46/97.52	97.31/97.39	96.44/96.61
	ReLU	46.72/47.80	96.68/96.78	94.68/94.68	97.98/97.98	97.78/97.89	97.59/97.74
	Tanh	43.07/45.90	95.17/96.73	97.40/97.44	97.57/97.57	97.61/97.65	97.45/97.54
F05	LogS	89.10/90.01	91.01/91.69	96.88/96.90	96.41/97.51	95.80/96.93	95.01/95.59
	ReLU	x	x	x	x	95.61/97.29	96.49/97.63
	Tanh	x	x	x	79.79/90.40	96.15/96.21	96.41/97.19
F06	LogS	97.82/97.86	97.74/97.82	97.69/97.69	97.35/97.43	96.43/96.60	95.45/95.53
	ReLU	96.77/96.81	97.62/97.62	97.71/97.82	97.71/97.84	97.46/97.64	97.31/97.41
	Tanh	41.00/41.86	97.37/97.43	97.61/97.67	97.64/97.76	97.41/97.57	97.12/97.40
F07	LogS	97.99/97.99	97.76/97.89	97.74/97.74	97.34/97.43	96.69/96.75	95.36/95.44
	ReLU	96.46/96.48	97.94/97.97	97.77/97.81	98.05/98.12	97.67/97.72	97.44/97.55
	Tanh	45.75/49.80	96.91/97.43	97.79/97.79	97.53/97.61	97.34/97.47	97.25/97.28
F08	LogS	93.55/93.90	95.50/95.66	96.47/97.26	95.65/96.93	94.89/96.12	93.82/94.46
	ReLU	x	x	x	68.57/76.95	95.77/97.22	95.52/96.98
	Tanh	x	x	x	94.54/94.69	94.97/97.17	95.86/96.76
F09	LogS	95.03/96.85	95.79/96.98	95.42/96.05	93.98/94.53	92.81/93.02	90.64/90.83
	ReLU	91.13/91.29	96.38/97.46	95.66/97.32	96.20/96.80	94.81/95.53	93.06/93.62
	Tanh	96.55/96.61	95.80/97.07	96.72/97.21	95.73/96.49	94.49/95.11	93.66/93.79
F10	LogS	93.40/93.69	93.76/96.04	93.09/95.63	93.59/94.99	91.64/92.80	91.14/91.91
	ReLU	x	x	x	93.62/95.45	94.81/96.65	94.78/95.61
	Tanh	x	55.44/61.14	93.47/93.58	92.33/95.28	94.22/95.57	91.85/92.97
F11	LogS	x	x	x	x	61.06/72.77	x
	ReLU	x	x	x	x	x	x
	Tanh	x	x	x	76.36/88.92	79.61/88.04	78.72/86.42
F12	LogS	93.05/93.40	96.75/96.75	96.84/97.08	96.62/96.82	95.85/96.21	94.99/95.29
	ReLU	x	x	59.26/61.40	97.10/97.10	96.76/96.96	96.28/96.72
	Tanh	x	x	88.46/90.36	96.12/96.22	96.51/96.61	96.02/96.54
F13	LogS	92.81/93.33	96.22/96.29	96.55/96.80	96.53/96.90	96.14/96.53	95.24/95.55
	ReLU	x	x	73.58/77.64	96.46/96.53	96.47/96.83	96.51/96.94
	Tanh	x	x	87.93/91.68	95.58/95.61	96.41/96.80	95.92/96.22
F14	LogS	95.82/97.00	95.87/96.86	95.81/96.55	94.22/94.98	93.41/93.61	91.12/91.62
	ReLU	x	96.82/97.45	96.91/97.49	96.50/97.20	95.55/96.24	94.25/94.84
	Tanh	96.86/97.02	97.48/97.51	96.59/97.21	96.08/96.82	94.70/95.62	93.36/93.79
F15	LogS	94.15/94.32	93.72/94.65	91.99/92.96	89.38/90.58	x	x
	ReLU	x	81.87/89.81	91.74/94.44	91.03/92.79	90.90/91.74	87.08/88.06
	Tanh	94.38/94.60	94.70/96.09	93.69/95.04	93.63/94.34	91.79/91.92	88.86/89.02
F16	LogS	95.44/96.76	96.29/96.92	95.96/96.40	94.86/95.11	93.18/93.56	90.81/91.22
	ReLU	x	96.19/97.54	96.04/97.56	96.26/97.07	95.33/95.92	94.25/94.75
	Tanh	97.14/97.18	96.29/97.20	96.79/97.30	96.25/97.02	94.84/95.59	93.24/93.61
F17	LogS	93.76/96.02	95.65/96.54	95.93/96.36	95.36/95.83	93.96/94.38	92.16/92.67
	ReLU	95.21/95.32	x	94.68/96.29	94.36/95.05	92.17/92.98	91.62/91.86
	Tanh	96.79/96.83	96.35/97.24	96.83/97.34	96.89/96.97	95.87/95.97	94.72/94.98
F18	LogS	97.16/97.47	97.11/97.37	96.65/96.89	95.60/95.78	94.24/94.49	92.06/92.22
	ReLU	97.51/97.51	97.60/97.60	97.14/97.53	96.97/97.28	96.11/96.13	95.03/95.13
	Tanh	96.71/96.73	96.91/97.09	97.02/97.16	96.30/96.56	96.20/96.23	94.65/94.74
F19	LogS	96.14/96.22	94.68/96.84	95.76/96.50	95.52/96.27	94.25/94.72	92.72/93.04
	ReLU	x	96.45/96.51	94.55/96.27	94.03/94.99	92.54/92.98	91.58/92.05
	Tanh	96.64/96.88	97.12/97.12	97.01/97.43	96.91/97.03	96.05/96.26	95.19/95.33
F20	LogS	97.67/97.88	96.97/97.32	96.71/97.16	95.81/96.10	94.67/94.89	92.97/93.23
	ReLU	83.72/89.56	97.87/97.90	96.76/97.65	96.69/97.33	96.57/96.70	94.71/94.84
	Tanh	x	97.21/97.28	97.04/97.47	96.94/97.22	96.28/96.44	95.00/95.04

Table 7: Full Results on MNIST — 5 Hidden Layers

ID	Act.	$\gamma = 0$	$\gamma = -1$	$\gamma = -2$	$\gamma = -3$	$\gamma = -4$	$\gamma = -5$
F01	LogS	92.42/94.82	93.77/95.55	94.55/95.78	93.04/94.42	90.54/91.96	86.72/88.39
	ReLU	x	x	x	95.82/96.04	92.83/94.14	91.14/92.58
	Tanh	x	95.47/95.72	96.04/96.61	96.27/96.80	95.26/95.77	93.92/94.45
F02	LogS	94.47/95.41	93.42/95.10	91.74/93.86	90.25/92.14	x	x
	ReLU	x	79.09/90.11	96.10/96.39	94.15/95.48	92.05/93.67	89.13/91.50
	Tanh	95.20/95.28	95.93/96.40	95.75/96.30	95.25/95.75	93.46/94.18	91.01/91.82
F03	LogS	97.90/97.92	97.99/97.99	98.08/98.10	97.66/97.67	97.29/97.41	96.47/96.59
	ReLU	x	x	x	x	x	91.69/91.69
	Tanh	x	x	97.78/97.78	97.92/97.92	97.84/97.85	97.79/97.82
F04	LogS	97.69/97.71	97.72/97.72	97.73/97.78	97.61/97.72	97.60/97.64	96.83/96.99
	ReLU	x	x	x	x	x	89.49/89.49
	Tanh	x	x	97.59/97.59	97.79/97.80	97.90/97.93	97.63/97.63
F05	LogS	87.68/88.71	91.20/91.65	96.73/97.07	97.45/97.55	96.49/97.00	95.05/95.72
	ReLU	x	x	x	x	95.20/95.93	95.50/96.22
	Tanh	x	x	x	x	x	x
F06	LogS	97.79/97.85	97.81/97.81	97.71/97.73	97.44/97.48	96.85/96.93	95.43/95.48
	ReLU	x	x	x	97.70/97.70	x	97.30/97.39
	Tanh	51.02/51.02	97.50/97.50	97.60/97.60	97.54/97.63	97.91/97.91	97.55/97.58
F07	LogS	97.92/97.92	97.79/97.79	97.67/97.74	97.59/97.64	96.66/96.73	95.49/95.61
	ReLU	x	x	x	x	97.58/97.58	97.31/97.33
	Tanh	x	97.63/97.63	97.66/97.66	97.75/97.79	97.52/97.54	97.41/97.41
F08	LogS	93.90/94.24	95.61/95.88	97.41/97.56	96.96/97.27	96.03/96.36	94.17/94.58
	ReLU	x	x	x	92.35/92.97	97.30/97.37	97.30/97.35
	Tanh	x	x	x	95.53/96.13	97.40/97.46	97.29/97.34
F09	LogS	95.97/96.24	95.75/96.28	94.95/95.58	93.75/94.34	90.07/91.51	80.88/86.51
	ReLU	92.43/92.76	97.15/97.32	97.39/97.54	96.85/96.85	95.48/95.79	93.60/93.89
	Tanh	96.17/96.52	96.45/96.73	96.92/96.98	96.53/96.63	95.24/95.64	92.85/93.39
F10	LogS	91.86/93.49	93.66/95.44	93.00/94.78	90.78/93.13	84.66/88.50	78.85/83.61
	ReLU	x	x	x	96.60/96.89	96.64/96.82	95.13/95.67
	Tanh	x	x	94.03/94.12	95.76/95.94	95.27/95.58	93.26/94.04
F11	LogS	x	x	x	x	x	x
	ReLU	x	x	x	x	x	x
	Tanh	x	x	x	86.25/87.94	84.39/86.63	82.31/85.15
F12	LogS	91.56/91.56	96.04/96.04	96.83/96.83	96.31/96.33	96.55/96.55	95.92/95.98
	ReLU	x	x	x	93.51/93.51	93.62/93.62	93.04/93.04
	Tanh	x	x	88.65/88.65	95.33/95.33	96.13/96.13	95.62/95.62
F13	LogS	91.06/91.06	95.91/95.91	96.44/96.44	96.35/96.39	96.13/96.13	96.10/96.10
	ReLU	x	x	x	94.03/94.03	93.74/93.74	93.45/93.45
	Tanh	x	x	87.31/87.31	95.10/95.10	95.91/95.91	95.65/95.65
F14	LogS	96.62/96.85	96.68/96.97	96.16/96.32	94.39/94.87	91.31/92.49	88.04/89.99
	ReLU	x	x	x	x	x	x
	Tanh	96.31/96.91	97.20/97.25	97.35/97.41	96.89/96.97	95.96/96.01	93.97/94.15
F15	LogS	87.41/92.13	87.68/93.17	84.54/90.67	x	x	x
	ReLU	x	x	x	90.21/90.21	88.93/88.93	x
	Tanh	94.19/94.19	95.45/96.00	94.33/95.34	91.79/93.14	89.10/91.01	83.06/86.23
F16	LogS	96.28/96.53	96.72/96.73	96.25/96.65	94.61/94.82	91.40/92.44	87.13/89.47
	ReLU	x	97.22/97.33	97.40/97.44	97.37/97.47	95.98/96.24	94.36/94.80
	Tanh	96.33/96.51	96.84/97.01	97.32/97.38	96.46/96.68	95.64/95.70	93.18/93.82
F17	LogS	91.95/94.24	93.98/95.37	94.55/95.21	93.48/94.77	91.67/92.94	87.56/88.93
	ReLU	x	x	x	x	x	x
	Tanh	63.88/93.22	67.87/95.10	78.94/95.57	84.23/95.79	85.49/94.42	81.06/93.23
F18	LogS	96.66/96.73	96.60/96.81	96.30/96.47	95.08/95.44	92.93/93.78	89.06/91.47
	ReLU	x	x	x	x	x	x
	Tanh	61.54/95.91	61.73/96.20	73.97/95.78	81.92/95.73	84.87/94.35	82.47/93.99
F19	LogS	x	94.33/96.41	95.27/95.88	93.67/94.87	92.09/93.13	88.87/89.68
	ReLU	x	x	x	x	x	x
	Tanh	x	96.02/96.02	95.60/96.52	95.91/96.15	94.99/95.91	94.13/94.67
F20	LogS	97.24/97.25	97.02/97.04	96.68/96.85	95.74/95.97	94.00/94.59	91.13/92.20
	ReLU	x	x	x	x	x	x
	Tanh	x	96.72/96.72	96.38/96.56	96.05/96.57	95.59/96.00	94.41/95.02

Table 8: Full Results on MNIST — 10 Hidden Layers

ID	Act.	$\gamma = 0$	$\gamma = -1$	$\gamma = -2$	$\gamma = -3$	$\gamma = -4$	$\gamma = -5$
F01	LogS	90.33/92.32	91.96/94.73	93.48/95.08	92.01/93.72	89.92/91.79	83.04/87.84
	ReLU	x	x	x	95.81/95.91	92.03/93.45	90.69/91.97
	Tanh	x	95.04/95.04	95.70/96.10	95.76/96.28	94.96/95.66	93.03/94.26
F02	LogS	93.63/93.79	93.14/94.92	91.84/93.55	88.80/91.46	x	x
	ReLU	x	x	96.07/96.65	95.14/95.74	92.92/93.68	91.06/92.05
	Tanh	95.34/95.34	95.85/95.85	95.63/96.24	94.59/95.56	92.96/94.05	90.61/91.69
F03	LogS	97.63/97.63	97.77/97.77	97.85/97.85	97.59/97.65	97.22/97.41	96.67/96.86
	ReLU	x	x	x	x	x	x
	Tanh	x	x	97.70/97.70	97.83/97.85	97.84/97.87	97.65/97.67
F04	LogS	97.40/97.45	97.78/97.78	97.65/97.70	97.53/97.62	97.40/97.51	96.74/96.86
	ReLU	x	x	x	x	x	x
	Tanh	x	x	97.82/97.82	97.71/97.72	97.44/97.44	97.66/97.69
F05	LogS	81.21/81.21	91.34/92.20	96.73/97.05	97.11/97.52	96.11/96.71	94.47/95.21
	ReLU	x	x	x	x	93.04/93.04	95.15/95.92
	Tanh	x	x	x	x	x	x
F06	LogS	97.86/97.94	98.08/98.08	97.78/97.80	97.36/97.45	96.73/96.92	94.92/95.17
	ReLU	x	x	x	x	x	97.50/97.55
	Tanh	x	97.59/97.59	97.54/97.60	97.69/97.70	97.44/97.45	97.24/97.26
F07	LogS	97.71/97.71	98.09/98.09	97.64/97.73	97.51/97.57	96.65/96.82	95.17/95.34
	ReLU	x	x	x	x	97.64/97.72	97.50/97.50
	Tanh	x	97.30/97.31	97.55/97.62	97.63/97.63	97.71/97.73	97.39/97.40
F08	LogS	93.68/94.10	96.11/96.16	97.38/97.45	96.88/97.07	95.82/96.05	93.68/94.31
	ReLU	x	x	x	73.04/77.96	97.26/97.27	97.27/97.27
	Tanh	x	x	x	95.84/96.19	97.29/97.53	97.41/97.53
F09	LogS	95.83/96.11	95.67/96.59	94.87/95.52	93.21/94.16	90.31/91.91	82.49/87.59
	ReLU	91.71/91.71	96.96/97.31	96.96/97.03	96.67/96.98	95.06/95.51	92.88/93.60
	Tanh	95.47/95.47	96.47/96.85	96.84/97.00	95.87/96.27	95.10/95.60	92.81/93.52
F10	LogS	91.58/92.36	94.68/95.53	91.84/94.42	90.79/93.02	79.73/84.32	62.24/70.82
	ReLU	x	x	x	94.97/95.25	96.66/96.94	94.86/95.27
	Tanh	x	x	94.87/94.97	95.49/95.85	93.75/94.03	93.76/94.12
F11	LogS	x	x	x	x	x	x
	ReLU	x	x	x	x	x	x
	Tanh	x	x	x	83.86/83.86	84.83/86.49	81.61/84.68
F12	LogS	91.84/91.84	96.18/96.18	96.52/96.52	96.49/96.49	96.32/96.32	95.64/95.64
	ReLU	x	x	x	91.39/91.39	91.63/91.63	90.70/90.70
	Tanh	x	x	85.67/85.67	94.96/94.96	95.26/95.26	95.13/95.13
F13	LogS	90.84/90.84	95.91/95.91	96.84/96.84	96.50/96.50	96.25/96.25	95.97/95.97
	ReLU	x	x	x	92.20/92.20	92.08/92.08	90.73/90.73
	Tanh	x	x	86.73/86.73	94.47/94.47	95.36/95.36	95.22/95.22
F14	LogS	96.50/96.83	96.42/96.73	95.48/95.96	94.46/94.76	90.75/92.57	86.01/89.92
	ReLU	x	x	x	x	x	x
	Tanh	96.09/96.09	96.74/97.05	97.09/97.37	96.84/97.05	95.26/95.57	93.32/93.95
F15	LogS	88.76/88.76	86.05/86.05	83.40/90.20	x	x	x
	ReLU	x	x	x	x	x	x
	Tanh	92.89/92.89	94.12/94.12	93.47/93.47	91.73/92.73	88.37/90.77	82.29/85.08
F16	LogS	95.98/96.45	96.22/96.70	95.56/95.97	93.60/94.23	90.56/91.89	84.16/88.88
	ReLU	x	97.33/97.45	97.22/97.25	97.11/97.23	95.91/96.32	93.52/94.26
	Tanh	96.39/96.39	96.49/96.68	96.88/97.13	96.43/96.68	95.08/95.47	93.25/93.77
F17	LogS	90.20/90.20	93.24/94.46	93.44/95.21	92.86/94.12	89.86/91.93	85.66/86.88
	ReLU	x	x	x	x	x	x
	Tanh	x	x	x	71.84/95.60	74.99/94.36	67.85/92.86
F18	LogS	96.34/96.65	96.40/96.84	96.12/96.70	94.85/95.51	91.49/92.95	87.64/90.82
	ReLU	x	x	x	x	x	x
	Tanh	x	x	46.90/95.71	60.29/95.82	72.18/95.21	67.11/93.56
F19	LogS	x	92.27/93.91	93.20/94.08	93.75/94.80	90.26/92.94	87.45/89.11
	ReLU	x	x	x	x	x	x
	Tanh	x	95.44/95.44	95.28/95.28	95.20/95.20	94.68/95.21	92.56/93.86
F20	LogS	97.12/97.39	97.11/97.41	96.30/96.74	95.16/95.77	93.09/94.33	89.18/90.91
	ReLU	x	x	x	x	x	x
	Tanh	x	96.03/96.03	95.75/95.75	95.96/95.96	95.03/95.43	92.59/93.79